International Journal of Nanomedicine

Dovepress
open access to scientific and medical research

Open Access Full Text Article

ORIGINAL RESEARCH

Folic acid-functionalized polyethylenimine superparamagnetic iron oxide nanoparticles as theranostic agents for magnetic resonance imaging and PD-L1 siRNA delivery for gastric cancer

This article was published in the following Dove Press journal:
International Journal of Nanomedicine
26 July 2017
Number of times this article has been viewed

Xin Luo[1,*]
Xia Peng[1,*]
Jingying Hou[2]
Shuyun Wu[3]
Jun Shen[4]
Lingyun Wang[1]

[1]Department of Gastroenterology, [2]Department of Emergency Medicine, Sun Yat-sen Memorial Hospital, [3]Department of Thoracic Surgery, Sun Yat-sen University Cancer Center, [4]Department of Radiology, Sun Yat-sen Memorial Hospital, Sun Yat-sen University, Guangzhou, China

*These authors contributed equally to this work

Abstract: Programmed death ligand-1 (PD-L1), which is highly expressed in gastric cancers, interacts with programmed death-1 (PD-1) on T cells and is involved in T-cell immune resistance. To increase the therapeutic safety and accuracy of PD-1/PD-L1 blockade, RNA interference through targeted gene delivery was performed in our study. We developed folic acid (FA)- and disulfide (SS)–polyethylene glycol (PEG)-conjugated polyethylenimine (PEI) complexed with superparamagnetic iron oxide Fe_3O_4 nanoparticles (SPIONs) as a siRNA-delivery system for PD-L1 knockdown. The characterization, binding ability, cytotoxicity, transfection efficiency, and cellular internalization of the polyplex were determined. At nitrogen:phosphate (N:P) ratios of 10 or above, the FA-PEG-SS-PEI-SPIONs bound to PD-L1 siRNA to form a polyplex with a diameter of approximately 120 nm. Cell-viability assays showed that the polyplex had minimal cytotoxicity at low N:P ratios. The FA-conjugated polyplex showed higher transfection efficiency and cellular internalization in the folate receptor-overexpressing gastric cancer cell line SGC-7901 than a non-FA-conjugated polyplex. Subsequently, we adopted the targeted FA-PEG-SS-PEI-SPION/siRNA polyplexes at an N:P ratio of 10 for function studies. Cellular magnetic resonance imaging (MRI) showed that the polyplex could also act as a T_2-weighted contrast agent for cancer MRI. Furthermore, one of four PD-L1 siRNAs exhibited effective PD-L1 knockdown in PD-L1-overexpressing SGC-7901. To determine the effects of the functionalized polyplex on T-cell function, we established a coculture model of activated T cells and SGC-7901 cells and demonstrated changes in secreted cytokines. Our findings highlight the potential of this class of multifunctional theranostic nanoparticles for effective targeted PD-L1-knockdown therapy and MRI diagnosis in gastric cancers.

Keywords: magnetic resonance imaging, theranostics, RNA interference, PEI, cellular internalization

Correspondence: Jun Shen
Department of Radiology Sun Yat-sen Memorial Hospital, Sun Yat-sen University, 107 Yanjiang Xi Road, Guangzhou, Guangdong 510120, China
Tel +86 20 8133 2243
Email shenjun@mail.sysu.edu.cn

Lingyun Wang
Department of Gastroenterology, Sun Yat-sen Memorial Hospital, Sun Yat-sen University, 107 Yanjiang Xi Road, Guangzhou, Guangdong 510120, China
Tel +86 20 8133 2309
Email xzr020@aliyun.com

Introduction

Gastric cancer (GC) is the third-most prevalent cause of all cancer deaths and has the highest incidence rate and mortality among some Asian, Eastern European, and Latin American countries.[1,2] For patients in locally advanced or metastatic stages who have lost the opportunity for surgery, chemotherapy is the best treatment option. However, the development of chemoresistance and the toxicity of chemotherapy have limited its therapeutic efficacy. To meet the need to explore new therapies for GC, therapeutic targets, such as immune checkpoints, have recently gained attention. PD-L1, which binds to PD-1 expressed on the surface of activated T cells, takes part in surveillance escape by immune

submit your manuscript | www.dovepress.com
Dovepress
http://dx.doi.org/10.2147/IJN.S137245

cells in cancers.[3] As a ligand widely expressed on tumor cells and tumor stroma, as well as healthy cells, PD-L1 can inhibit T-cell responses by promoting the induction and maintenance of T-regulatory (T_{reg}) cells[4] and by binding to the costimulatory molecule B7-1.[5,6] Moreover, high expression of PD-1/PD-L1 is observed in GC tissues,[7–9] and for advanced GC patients, PD-L1 has been shown to be an indicator of worse prognosis.[10–15] Furthermore, the pattern of PD-L1 overexpression is also characterized by a molecular subtype of GC according to the Cancer Genome Atlas Research Network.[16] Given that PD-L1 plays a pivotal role in the progression of GC, blocking the interaction of PD-1/PD-L1 would have significant potential to reverse immunoescape and improve the prognosis of patients.

In recent studies, monoclonal antibodies blocking the PD-1/PD-L1 interaction have been investigated, while blockade using RNA interference (RNAi) with nanocarriers is rare. RNAi is a promising strategy for therapeutic gene silencing. Through RNAi, targeted protein expression is safely knocked down at post-transcriptional levels without inserting exogenous sequences into the genome. Corresponding mRNA is specifically targeted by the RNA-induced silencing complex, formed in the cytoplasm by double-stranded siRNAs. The major hurdles of this mechanism are that siRNA can easily be degraded by enzymes in physiological circumstances and that the intrinsic negative charge prevents siRNA from penetrating the cellular membrane. To overcome these drawbacks, polymer nanocarriers have been utilized as siRNA-delivery agents. PD-L1-targeted siRNA was transported to PD-L1/folate receptor (FR)-overexpressing GC SGC-7901 cells for PD-L1 knockdown.[17] Among the nonviral gene-delivery systems, using polyethylenimine (PEI) leads to the highest transfection efficiency in vitro. With a high cationic charge density, this polycation can bind negatively charged siRNA. Most importantly, via the "proton sponge" effect, second and tertiary amines on PEI are able to buffer protons in the endosomes,[18,19] enabling PEI/siRNA polyplexes to escape lysosomal degradation. However, PEI with high cationic charge densities also exhibits great cytotoxicity. In this regard, we modified PEI with disulfide (SS)-conjugated polyethylene glycol (PEG). PEG modification lowers cytotoxicity and increases stabilization before cellular internalization. In addition, the SS bond enables glutathione-sensitive release of PEI siRNA in the cytoplasm, which enhances the efficacy of siRNA delivery. A wide range of tumors, such as ovary, kidney, colon, breast, and lung cancers, overexpress FRs.[20,21] Folic acid (FA), an oxidized form of folate, can bind to FRs and increase cellular uptake, which makes it a specific ligand to target FR-overexpressing cancers. In addition, superparamagnetic iron oxide Fe_3O_4 (SPIO) has been encapsulated with a delivery agent for its known capacity as a T_2-weighted contrast agent for magnetic resonance imaging (MRI). Tumor-targeting ability, minimal toxicity, stability outside the cell membrane, accurate siRNA release in the cytoplasm, and MR-tracing ability makes the nanoparticle an effective therapeutic agent for treatment of PD-L1-positive GC. MR-tracing ability is measured using in vitro MRI, and knockdown efficiency measured with quantitative reverse-transcription polymerase chain reaction (qRT-PCR) and Western blotting. To perform function experiments, we established a coculture model of SGC-7901 cells and T cells, and cytokines in the coculture medium were measured using an enzyme-linked immunosorbent assay (ELISA). To the best of our knowledge, our work is the first to perform a PD-1/PD-L1-checkpoint blockade in GC cells through delivery of PD-L1 siRNA transported via FA-PEG-modified PEI polymers.

Materials and methods

Materials

Most of the chemical reagents, including PEI (molecular weight [MW] 25 kDa), monomethoxy-PEG (mPEG-OH; 2 kDa), succinic anhydride, dicyclohexylcarbodiimide (DCC), and *N*-hydroxysuccinimide (NHS), were obtained from Sigma-Aldrich Co. (St Louis, MO, USA). Hydrophobic SPIO nanoparticles (SPIONs) measuring 6 nm in diameter on average were synthesized following a previously reported method with minor modifications.[22] α-Hydroxy-ε-amino-PEG (HO-PEG-NH_2; number-average molar mass [M_n] 3.6 kDa, MW/M_n=1.3) was prepared according to a previously described method with minor modifications.[23] PD-L1 and scrambled siRNA (siScr) were purchased from GenePharma (Suzhou, China). The siRNA sequences were as follows: siRNA1, (sense) 5′-GGAUCCAGUCACCUCUGAATT-3′ and (antisense) 5′-UUCAGAGGUGACUGGAUCCTT-3′; siRNA2, (sense) 5′-CCAGCACACUGAGAAUCAATT-3′ and (antisense) 5′-UUGAUUCUCAGUGUGCUGGTT-3′; siRNA3, (sense) 5′-GGCACAUCCUCCAAAUGAATT-3′ and (antisense) 5′-UUCAUUUGGAGGAUGUGCCTT-3′; siRNA4, (sense) 5′-GGAGAAUGAUGGAUGUGAATT-3′ and (antisense) 5′-UUCACAUCCAUCAUUCUCCTT-3′; and siScr, (sense) 5′-UUCUCCGAACGUGUCACGUTT-3′ and (antisense) 5′-ACGUGACACGUUCGGAGAATT-3′. Human IL10/IFNγ/TNFα/CCL22 ELISA kits were purchased from Thermo Fisher Scientific (Waltham, MA, USA). qPCR primers (PD-L1, sense 5′-GTGGCATCCAAGATACAAACTCAA-3′ and antisense 5′-TCCTTCCTCTTGTCACGCTCA-3′; GAPDH, sense 5′-ATGGGGAAGGTGAAGGTCG-3′ and

antisense 5′-GGGTCATTGATGGCAACAATATC-3′) were purchased from BGI (Beijing, China). An RNAiso Plus kit, PrimeScript RT Master Mix, and SYBR Premix Ex Taq II were purchased from Takara Bio (Kusatsu, Japan). Histopaque-1077 was purchased from Sigma-Aldrich Co. The human GC cell line SGC-7901 was obtained from the Institute of Biochemistry and Cell Biology, Chinese Academy of Sciences (Shanghai, China) and grown in folate-free RPMI 1640 medium supplemented with 10% fetal bovine serum (FBS) and 5% L-glutamine–penicillin–streptomycin solution (Sigma-Aldrich Co.). Activated T cells were grown in T-cell medium (RPMI 1640 supplemented with 10% heat-inactivated FBS, 5% L-glutamine–penicillin–streptomycin solution).

Synthesis of delivery agents

The FA-PEG-SS-PEI block copolymer was synthesized and activated according to a previously described method with minor modifications.[24] Briefly, to conjugate folate to HO-PEG-NH_2,[25] FA was dissolved in anhydrous dimethyl sulfoxide (DMSO; 20 mL). NHS and dicyclohexylcarbodiimide (DCC) were added, and the mixture was stirred overnight at room temperature. Then, under an argon atmosphere, the mixture was filtered using a 0.22 µm filter to remove the by-product 1,3-dicyclohexylurea (DCU), and the filtrate was mixed with a DMSO solution of HO-PEG-NH_2 containing triethylamine (pH 8). The mixture was reacted for 24 hours at room temperature, dialyzed against deionized water (MW cutoff [MWCO] 1,000 Da), and lyophilized. Then, 3-(2-carboxy-ethyldisulfanyl)-propionic acid, NHS, and dimethylaminopyridine (DMAP) were dissolved in anhydrous DMSO (20 mL), and the mixture was stirred overnight at room temperature. FA-PEG-OH was added and reacted for 24 hours. The mixture was dialyzed against deionized water (MWCO 1,000 Da) and lyophilized. Finally, the product, NHS, and DCC were dissolved in anhydrous DMSO (20 mL), and the mixture was stirred overnight at room temperature. Then, the mixture was filtered with a 0.22 µm filter head to remove the by-product DCU. Hyperbranched PEI was added to the mixture and reacted for 24 hours at room temperature to produce FA-PEG-SS-PEI. The mixture was purified using membrane dialysis (MWCO 14,000 Da) in distilled water for 3 days, and the solution was lyophilized (Figure 1A).

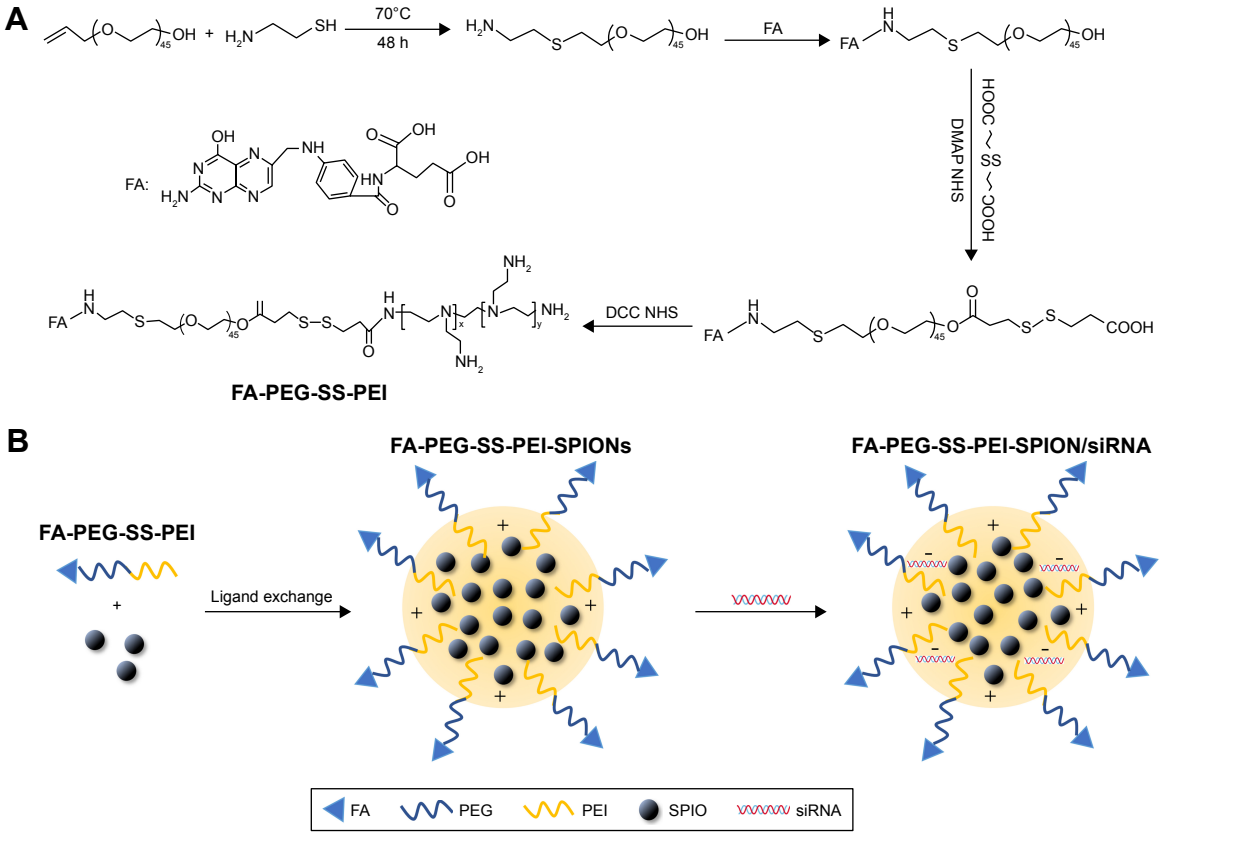

Figure 1 Polymer and polyplex preparation.
Notes: (**A**) Synthesis of FA-PEG-SS-PEI polymer; (**B**) formation of FA-PEG-SS-PEI-SPION/siRNA polyplex.
Abbreviations: FA, folic acid; PEG, polyethylene glycol; SS, disulfide; PEI, polyethylenimine; SPION, superparamagnetic iron oxide nanoparticle; DMAP, dimethylaminopyridine; NHS, *N*-hydroxysuccinimide; DCC, dicyclohexylcarbodiimide.

Nontargeting mPEG-SS-PEI was synthesized using the same approach.

Preparation of nanoparticles

SPIONs encapsulated with FA-PEG-SS-PEI or mPEG-SS-PEI were prepared by a ligand-exchange method as reported in the literature.[26] FA-PEG-SS-PEI or mPEG-SS-PEI (200 mg) was dissolved in 2 mL of chloroform, and then SPIONs (10 mg) were dispersed into the solution. The reaction mixture was stirred overnight at room temperature and then precipitated in a large amount of hexane. The precipitate was collected by centrifugation, washed twice with hexane, and vacuum-dried to remove organic solvent. The product thus prepared was dispersed into double-distilled water under sonication and filtered through a 220 nm membrane to remove large aggregates.

Preparation of siRNA-complexed cationic micelles

siRNA (4 mg) and an appropriate amount of delivery agent were dissolved separately in RNase-free water for gel-electrophoresis assay or folate-free RPMI 1640 medium for transfection assays. The two solutions were mixed by vigorous pipetting, and then, the mixture was maintained at room temperature for 60 minutes to allow complete polyplex formation. The amount of delivery agent used to complex siRNA was determined based on the designed experimental nitrogen:phosphate (N:P) ratios, which were calculated as the number of nitrogen atoms in delivery agents over those of the phosphate groups in siRNA. For cellular transfection, the polyplex was diluted to a siRNA concentration of 50 nM in cell-culture medium. The formation procedure of siRNA-complexed cationic micelles is summarized in Figure 1B.

Particle size and ζ-potential measurements

PD-L1 siRNA was complexed with modified PEI in RNase-free water at various N:P ratios. After mixing diluted siRNA solution with diluted polymer solution, the mixture was incubated for 1 hour at room temperature and then diluted again using RNase-free water. Particle size and ζ-potential were measured by dynamic light scattering using a Zetasizer Nano (Malvern Instruments, Malvern, UK). Scattered light was detected at a temperature of 25°C and an angle of 90°. All measurements were repeated at least three times per sample, and results are presented as mean ± standard deviation.

Agarose-gel electrophoresis

The binding ability of FA-PEG-SS-PEI-SPIONs and PEG-SS-PEI-SPIONs with siRNA was determined with agarose-gel electrophoresis. Complexes of PEG-SS-PEI-SPION/siRNA and FA-PEG-SS-PEI-SPION/siRNA were formed by mixing human siScr (GenePharma) and PEG-SS-PEI-SPIONs or FA-PEG-SS-PEI-SPIONs at various N:P ratios in deionized RNase-free water. The amount of siRNA was set at 10 pmol for each sample. Complexes were subsequently incubated for 1 hour at room temperature to form polyplexes. Then, polyplexes were mixed with 6× agarose-gel loading buffer and loaded onto 1% (w/v) agarose gels and run with Tris borate–EDTA running buffer at 100 V for 20 minutes. The siRNA bands were visualized with an ultraviolet-imaging system (Tanon, Shanghai, China).

Cytotoxicity of polymer/siRNA complexes

Cytotoxicity studies were performed using CellTiter 96® Aqueous One solution (MTS) assays (Promega Corporation, Fitchburg, WI, USA). SGC-7901 cells seeded in 96-well plates at 5×10^3 cells per well were treated with polymer/siScr complexes at a siRNA concentration of 100 nM. Then, at 72 hours post treatment, the polyplex medium was removed and the cells incubated for 3 hours at 37°C with MTS solution in cell-culture medium. Absorbance was read using a microplate spectrophotometer (Thermo Fisher Scientific) at wavelengths of 490 nm. Relative cell viability was calculated as (sample Abs_{490} − blank Abs_{490})/(control Abs_{490} − blank Abs_{490}) ×100%. Results are expressed as mean ± standard error of mean (SEM) of at least three replicates per N:P ratio from three independent experiments.

Flow cytometry

SGC-7901 cells were seeded in six-well plates at 2×10^5 cells per well. Polymer/5-carboxyfluorescein-(FAM)-labeled siScr polyplexes were complexed as described earlier at various N:P ratios and added to cultured cells at 100 pmol per well. Following 4 hours of incubation, the medium was replaced by PBS, and the cells were analyzed with a FACSVerse flow cytometer (Becton Dickinson, Franklin Lakes, NJ, USA). The proportion of FAM-positive cells was represented by transfection efficiency. The mean fluorescence index (MFI) was represented by geometric mean FAM absorbance.

Prussian blue staining

FA-PEG-SS-PEI-SPION or PEG-SS-PEI-SPION polymers contain iron oxide, and can be localized using Prussian blue staining. To confirm the cellular uptake of FA-PEG-SS-PEI-SPION/siRNA or the nontargeted polyplex, a Prussian blue staining experiment was conducted. First, SGC-7901 cells were incubated in polymer/siRNA at iron concentrations

of 0–40 μg/mL for 4 hours. Then, after removal of the transfection medium, cells were washed and fixed with 4% paraformaldehyde for 10 minutes at room temperature. Next, cells were washed again with PBS three times, and Prussian blue staining solution was added. After 30 minutes of incubation at room temperature, cells were washed three times with PBS and imaged under microscopy.

In vitro MRI

SGC-7901 cells were cultured in folate-free medium and treated with PEG-SS-PEI-SPION/siRNA or FA-PEG-SS-PEI-SPION/siRNA, respectively, at Fe concentrations of 0, 5, 10, 20, 40, and 80 μg/mL. SGC-7901 cells were harvested at 4 hours post-transfection and rinsed three times with PBS. After centrifugation, cells were resuspended in 500 μL of 1% (w/v) agarose/PBS solution and added to 96-well plates for MRI. Next, in vitro MRI was performed using a clinical 1.5 T system (Intera; Philips, Amsterdam, the Netherlands) with an 11 cm circular coil at room temperature.

Western blotting

SGC-7901 cells were seeded in six-well plates at 2×10^5 cells per well and transfected with polymer/siRNA as described earlier. Cells were harvested and lysed at 3 days post-transfection using radioimmunoprecipitation-assay lysis buffer (Santa Cruz Biotechnology, Dallas, TX, USA). Then, samples were run through 12% sodium dodecyl sulfate polyacrylamide gels and transferred onto polyvinylidene difluoride (PVDF) membranes. Monoclonal rabbit anti-PD-L1 antibody (Abcam, Cambridge, UK) and polyclonal rabbit anti-β-tubulin antibody (Cell Signaling Technology, Danvers, MA, USA) were used for Western blotting. Protein blots on PVDF membranes were imaged using a chemiluminescence-detection method (Merck Millipore, Billerica, MA, USA).

qRT-PCR analysis

SGC-7901 cells were seeded and transfected with polymer/siRNA as described earlier. RNA was extracted, purified, and converted to cDNA using the RNAiso Plus kit and PrimeScript RT Master Mix. qPCR was performed using SYBR Premix Ex Taq II on a CFX96 real-time PCR detection system (Bio-Rad Laboratories, Hercules, CA, USA) and analyzed using the $2^{-\Delta\Delta Cq}$ method. Results are expressed as mean ± SEM of three independent experiments.

Immunofluorescence analysis

SGC-7901 cells were seeded on 14 mm glass coverslips in 24-well plates at a density of 2×10^4 cells per slide and treated with FA-PEG-SS-PEI-SPION/PD-L1 siRNA2 polyplexes as described. At 3 days post-transfection, the cells were fixed with 4% paraformaldehyde for 10 minutes and washed three times with PBS. Next, goat serum was added and incubated for 30 minutes. After being washed three times with PBS, the cells were stained with rabbit anti-PD-L1 antibody. The cells were then washed three times and stained with Alexa Fluor 594 goat anti-rabbit secondary antibody (Thermo Fisher Scientific). Then, cells were washed three times with PBS, and DAPI was added for a 5-minute incubation. The cells were washed four times with PBS, mounted on a glass slide using ProLong Gold antifade mountant (Thermo Fisher Scientific), and imaged using laser-scanning confocal microscopy (AxioPlan 2; Carl Zeiss Meditec AG, Jena, Germany).

SGC-7901/T-cell coculture model

Written informed consent was obtained from participants, and the research was approved by the Sun Yat-sen Memorial Hospital's Research Ethics Committee. Peripheral blood mononuclear cells (PBMCs) from healthy human donors were isolated by Lymphoprep density-gradient centrifugation according to the manufacturer's instructions. Isolated PBMCs were seeded in 96-well plates at 2×10^5 cells per well and supplemented with anti-CD3e (10 mg/mL) and anti-CD28 (2 mg/mL) antibodies for 48 hours to stimulate T-cell activation. SGC-7901 cells were transfected with FA-PEG-SS-PEI-SPION/PD-L1 siRNA2 or FA-PEG-SS-PEI-SPION/siScr control for 4 hours. Activated PBMCs were then harvested and purified by Lymphoprep density-gradient centrifugation and cocultured with SGC-7901 cells at a ratio of 10:1 for 48 hours. Coculture media were assayed for CCL22, TNFα, IFNγ, and IL10 using cytokine ELISAs.

Statistical analysis

All experiments were performed at least in triplicate. Data are presented as mean ± SEM, and statistical analysis was performed using GraphPad Prism 5.0 (GraphPad Software Inc, La Jolla, CA, USA). Data were analyzed with two-tailed *t*-tests, and the differences were considered significant for $P<0.05$.

Results

Formation of mPEG-SS-PEI-SPION and FA-PEG-SS-PEI-SPION micelles

The synthesis of mPEG-SS-PEI and FA-PEG-SS-PEI was described in detail in the "Materials and methods" section. FA-PEG-SS-PEI-SPIONs and mPEG-SS-PEI-SPIONs were successfully synthesized by a ligand-exchange method. In this approach, the cationic copolymer mPEG-SS-PEI and FA-PEG-SS-PEI replaced the hydrophobic coating of

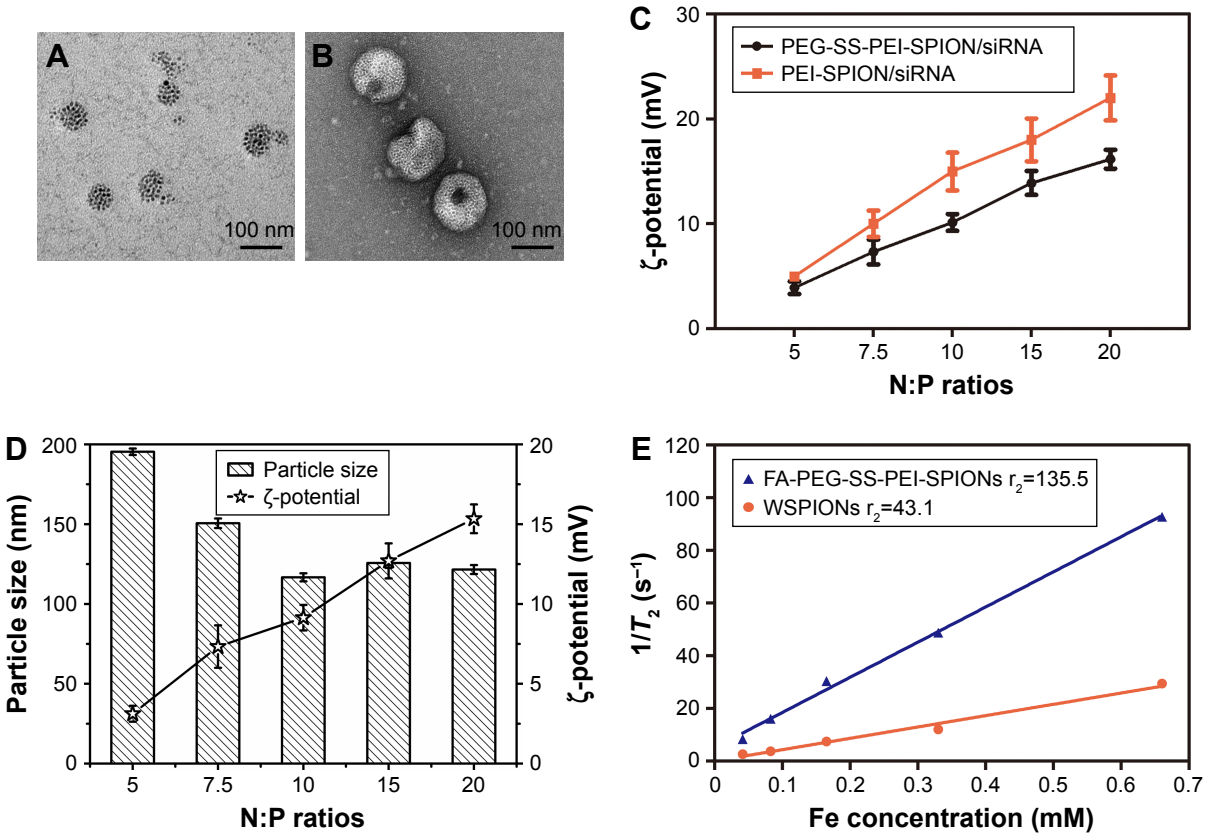

Figure 2 Morphology and characterization of FA-PEG-SS-PEI-SPIONs.
Notes: TEM of (**A**) FA-PEG-SS-PEI-SPIONs and (**B**) FA-PEG-SS-PEI-SPION/siRNA. (**C**) ζ-Potential of PEG-SS-PEI-SPION/siRNA and PEI-SPION/siRNA polyplexes at different N:P ratios. (**D**) ζ-Potential and particle size of FA-PEG-SS-PEI-SPION/siRNA at various N:P ratios. (**E**) T_2 relaxivities (r_2) of FA-PEG-SS-PEI-SPIONs and WSPIONs.
Abbreviations: FA, folic acid; PEG, polyethylene glycol; SS, disulfide; PEI, polyethylenimine; SPIONs, superparamagnetic iron oxide nanoparticles; TEM, transmission electron microscopy; N:P, nitrogen:phosphate; WSPIONs, water-soluble SPIONs.

oleic acid/oleylamine on the surface of SPIONs measuring 6 nm. The dispersion of the obtained complexes FA-PEG-SS-PEI-SPIONs and mPEG-SS-PEI-SPIONs in water was stable. Dynamic light-scattering measurements of the FA-PEG-SS-PEI–SPION complex in aqueous solution at room temperature showed an average hydrodynamic size of 58 nm (diameter), which was consistent with transmission electron microscopy (TEM) image data (Figure 2A).

Formation of mPEG-SS-PEI-SPION/FA-PEG-SS-PEI-SPION/siRNA complexes

The complexation of siRNA with cationic copolymers or micelles is due to electrostatic neutralization. To confirm the formation of FA-PEG-SS-PEI-SPION/siRNA complexes, we checked the retardation of siRNA mobility in agarose-gel electrophoresis. All copolymers started to form complexes from a low N:P ratio in this study (Figure 3). Compared with the naked siRNA control, all the copolymers showed

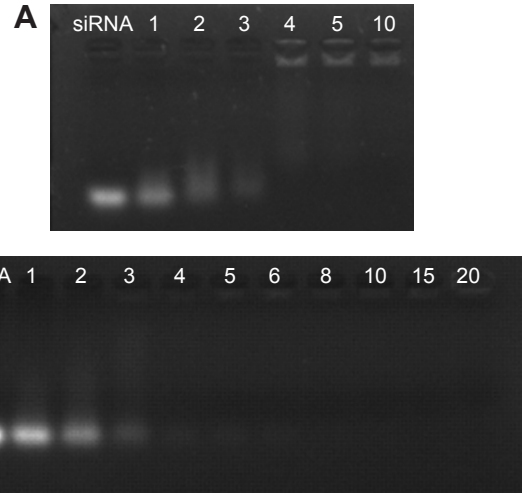

Figure 3 siRNA binding of PEG-SS-PEI-SPIONs and FA-PEG-SS-PEI-SPIONs.
Notes: Agarose-gel electrophoresis of (**A**) PEG-SS-PEI-SPION/siRNA and (**B**) FA-PEG-SS-PEI-SPION/siRNA at various N:P ratios. The control lane was naked siRNA.
Abbreviations: PEG, polyethylene glycol; SS, disulfide; PEI, polyethylenimine; SPIONs, superparamagnetic iron oxide nanoparticles; FA, folic acid; N:P, nitrogen:phosphate.

the capability of siRNA condensation as less siRNA ran into the gel. mPEG-SS-PEI-SPIONs exhibited better siRNA complexation, as siRNAs were almost completely retarded at an N:P ratio of 4, while some siRNA had not been complexed with FA-PEG-SS-PEI-SPIONs at N:P ratios of 4–6. At an N:P ratio of 10 or above, all the copolymers showed complete retardation of siRNA motion, indicating full siRNA complexation. PEG-SS-PEI-SPION/siRNA exhibited lower ζ-potentials versus PEI-SPION/siRNA at identical N:P ratios (Figure 2C). Upon siRNA complexation (N:P ratio 10), the mean diameter of the magnetic nanoparticles increased to approximately 120 nm (Figure 2D), which corresponded with the TEM image (Figure 2B). Moreover, the mean diameter was still an ideal size for cellular uptake and intravenous application. In addition, as shown in Figure 2E, the transverse relaxivity (r_2) values of the magnetic nanoparticles were measured to highlight the capability to enhance T_2-weighted contrast. The r_2 values were determined by the slope of the regression line of plots indicating $1/T_2$ (s^{-1}) versus Fe concentrations (mM). The r_2 of FA-PEG-SS-PEI-SPIONs was 135.5 $mM^{-1}\cdot s^{-1}$, much higher compared to hydrophilic SPIONs (water-soluble SPIONs, WSPIONs; r_2=43.1 $mM^{-1}\cdot s^{-1}$).

Cytotoxicity of polymer/siRNA complexes

The cytotoxicity of the polymer/siRNA polyplexes and the Lipofectamine 2000/siRNA lipoplex control was evaluated with MTS cell-viability assays. As shown in Figure 4, at low N:P ratios, both the FA-PEG-SS-PEI-SPION/siRNA and PEG-SS-PEI-SPION/siRNA polyplexes showed minimal cytotoxicity compared to the lipoplex control. As the N:P ratios rose, cell viability decreased from more than 95% to below 60%. With N:P ratios of 20 and below, the cell viability of SGC-7901 cells was higher than that of the Lipofectamine-treated cells at 72 hours post treatment with polyplex. In addition, the cytotoxicity of FA-PEG-SS-PEI-SPION/siRNA was as low as that of the PEG-SS-PEI-SPION/siRNA, which suggested good biocompatibility of the FA-conjugation modification.

Transfection efficiency

siScr-FAM was used to evaluate the transfection efficiency and quantify cellular uptake of PEG-SS-PEI-SPIONs and FA-PEG-SS-PEI-SPIONs in SGC-7901 cells via flow cytometry, with Lipofectamine 2000 used as the control. Transfection was conducted at siRNA concentrations of

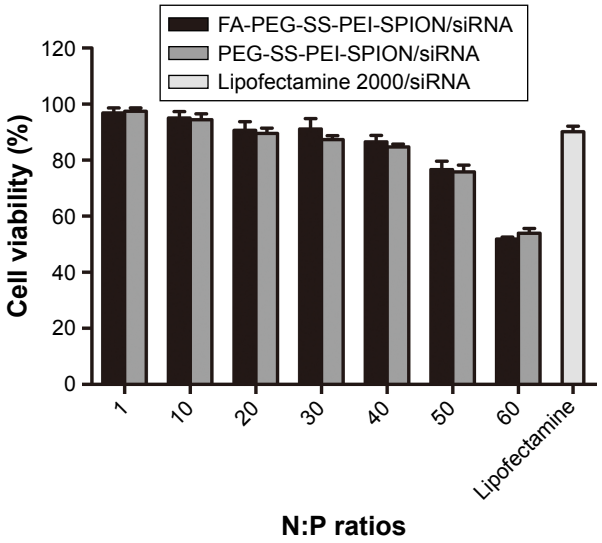

Figure 4 Cytotoxicity of PEG-SS-PEI-SPIONs and FA-PEG-SS-PEI-SPIONs.
Note: Viability of SGC-7901 cells treated with PEG-SS-PEI-SPION/siRNA, FA-PEG-SS-PEI-SPION/siRNA, or lipofectamine 2000/siRNA as control.
Abbreviations: PEG, polyethylene glycol; SS, disulfide; PEI, polyethylenimine; SPIONs, superparamagnetic iron oxide nanoparticles; FA, folic acid; N:P, nitrogen:phosphate.

50 nM for different N:P ratios. Cells that internalized the polymer/siRNA would be FAM-positive, and the MFI would represent the amount of cellular uptake.

At N:P ratios of 4 or 5, the transfection efficiency, or MFI, of FA-modified polyplexes was lower than that of the non-FA group, due to incomplete complexation with siRNA. At higher N:P ratios of 10 or 20, as the FA-modified polymers completely bound the siRNA and the transfection efficiency of the FA-modified polymers was as high as the non-FA polymer group (Figure 5A). However, the MFI was significantly higher for the FA-PEG-SS-PEI-SPIONs, indicating higher cellular internalization (Figure 5B). Therefore, at N:P ratios at which the polymers completely bind siRNA, both PEG-SS-PEI-SPIONs and FA-PEG-SS-PEI-SPIONs showed high transfection efficiency for in vitro transfection. In addition, the significantly high MFI showed that targeted FA conjugation was able to facilitate cellular internalization compared to nontargeted polyplex.

Cellular internalization of the polyplexes

To further visualize the cellular internalization of the polyplex, Prussian blue staining assays and confocal laser scanning were conducted. SPIONs can be stained blue by Prussian blue staining. Following gene transfection at an N:P ratio of 10, Prussian blue staining was performed to visualize the cellular uptake of the nanoparticles. At low iron concentrations (under 5 μg/mL), blue-stained particles

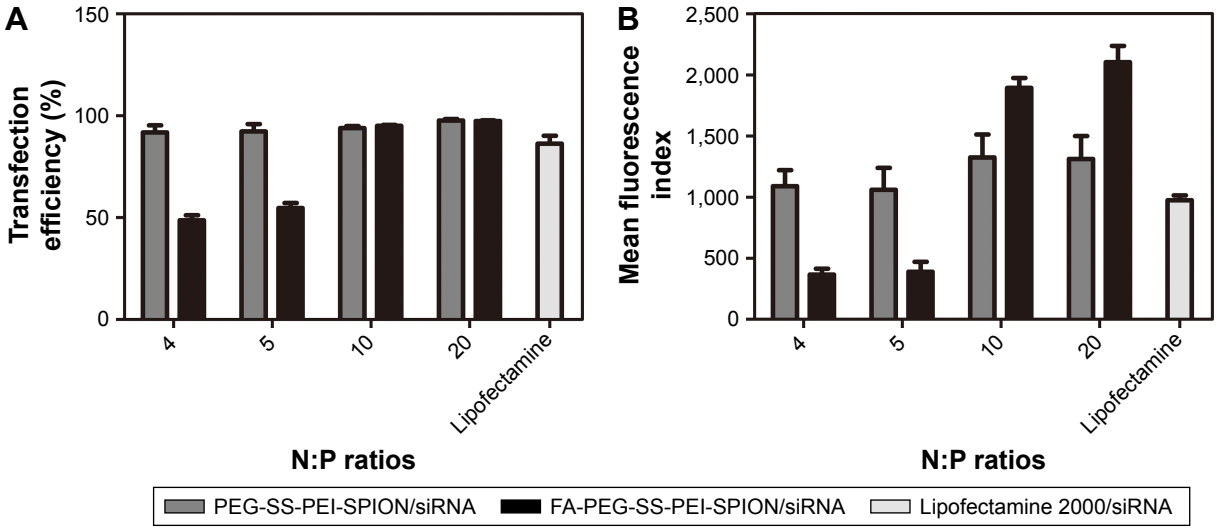

Figure 5 Transfection efficiency of PEG-SS-PEI-SPIONs and FA-PEG-SS-PEI-SPIONs.
Note: (**A**) Transfection efficiency and (**B**) mean fluorescence index of PEG-SS-PEI-SPION siRNA, FA-PEG-SS-PEI-SPION/siRNA, or Lipofectamine 2000/siRNA as control, determined by flow cytometry.
Abbreviations: PEG, polyethylene glycol; SS, disulfide; PEI, polyethylenimine; SPIONs, superparamagnetic iron oxide nanoparticles; FA, folic acid; N:P, nitrogen:phosphate.

were barely seen under microscopy (data not shown), while at 10 μg/mL or even higher iron concentrations, blue-stained particles appeared in the cytoplasm of most SGC-7901 cells (Figure 6A), which verified the internalization of the delivery agent containing SPIONs into the cells.

The uptake of the complexes was also visualized with confocal laser-scanning microscopy. In the cells treated with FA-PEG-SS-PEI-SPION/siScr-FAM, FAM green fluorescence was located in the perinuclear region of the cytoplasm. In addition, FA-PEG-SS-PEI-SPION/siScr-FAM treated cells internalized significantly more FAM green fluorescence than the non-FA-modified complex-treated cells (Figure 6B). This indicated that FA-PEG-SS-PEI-SPIONs delivered more siRNA into SGC-7901 cells than the nontargeting complex and have potential for better PD-L1 knockdown in vitro.

In vitro MRI

To evaluate the potential of the FA-PEG-SS-PEI-SPION as an MRI T_2-weighted contrast agent, SGC-7901 cells were incubated with folate-free medium supplemented with FA-PEG-SS-PEI-SPION/siRNA or PEG-SS-PEI-SPION/siRNA at various iron concentrations. After 4 hours of incubation, cells were harvested and added to 96-well plates as described in the "Materials and methods" section. As the iron concentration increased, the MRI T_2-signal intensity decreased post transfection with both PEG-SS-PEI-SPION/siRNA and FA-PEG-SS-PEI-SPION/siRNA (Figure 7A). An iron-concentration-dependent decrease in T_2 relaxation time was observed in both FP/siScr and PP/siScr treatment groups. In addition, SGC-7901 cells post-transfection with FA-PEG-SS-PEI-SPION/siRNA showed significantly lower T_2 values than with PEG-SS-PEI-SPION/siRNA at iron concentrations above 5 μg/mL (Figure 7B). Results of in vitro MRI indicated that both PEG-SS-PEI-SPIONs and FA-PEG-SS-PEI-SPIONs acted as T_2-weighted contrast agents and that FA-PEG-SS-PEI-SPION/siRNA was better than the other.

PD-L1 knockdown

To perform PD-L1 knockdown, PD-L1-targeted siRNAs were designed and examined using knockdown assays. A higher N:P ratio than 20 of the polyplexes increased cytotoxicity to SGC-7901 cells due to high cationic charge, according to the cytotoxicity assays. Considering a balance of low cytotoxicity and high transfection efficiency, an N:P ratio of 10 was used to complex siRNA and FA-PEG-SS-PEI-SPIONs.

qRT-PCR was performed to assess levels of PD-L1 mRNA expression. Among the four designed PD-L1-targeted siRNAs, siRNA1 and siRNA2 had an obvious effect, knocking down PD-L1 mRNA levels by 76.53%±4.59% and 90.93%±0.79%, respectively (Figure 8A). To further study whether PD-L1 expression on polymer/PD-L1 siRNA-treated SGC-7901 cells was lower than that on siScr-treated cells, Western blotting was conducted. PD-L1-expression levels on cells treated with polymer/siRNA were in accordance with the observed mRNA levels (Figure 8B). The FA-PEG-SS-PEI-SPION/PD-L1 siRNA2 polyplex had the most significant knockdown effect on PD-L1 protein

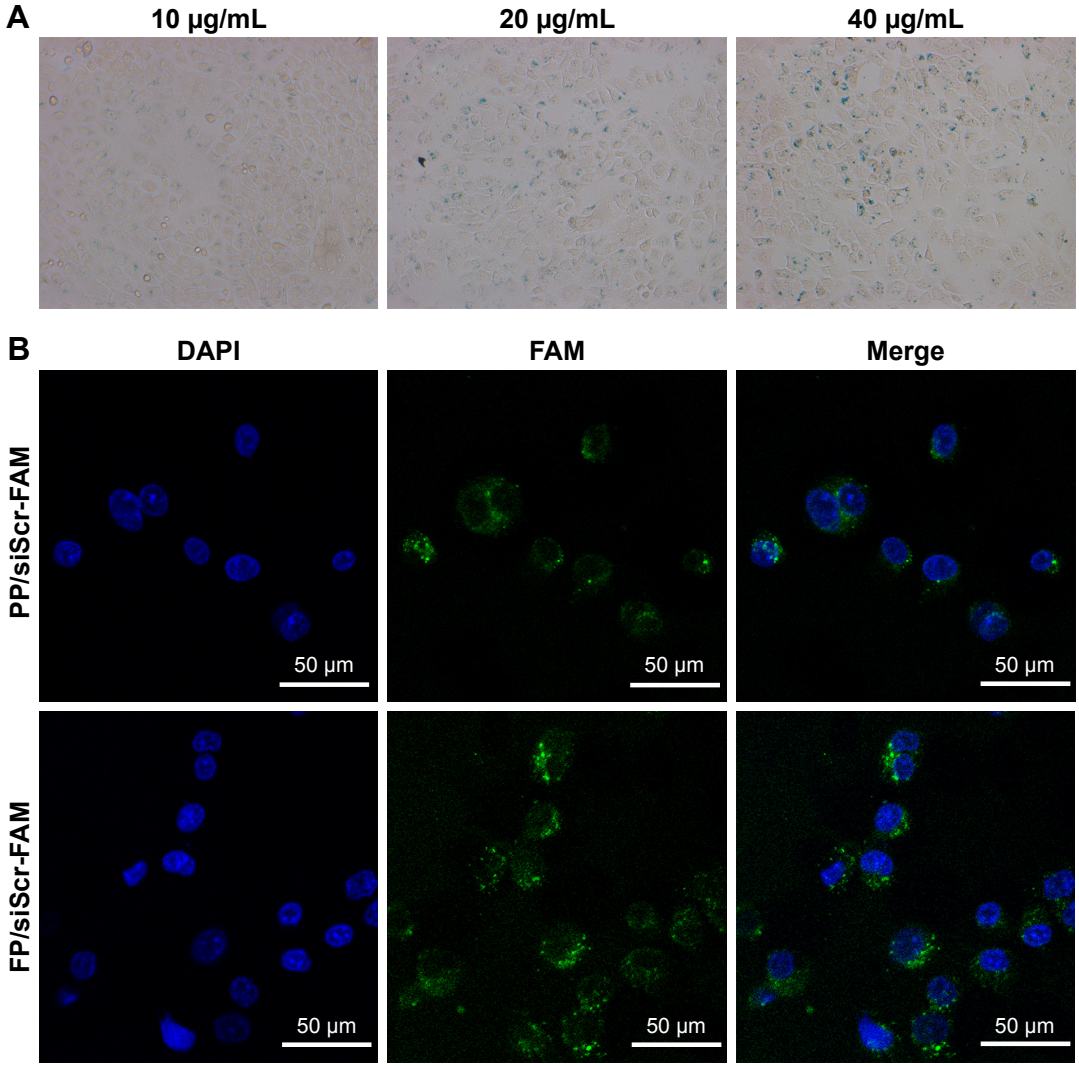

Figure 6 Cellular internalization of FA-PEG-SS-PEI-SPION/siRNA polyplex.
Notes: (**A**) Prussian blue staining of SGC-7901 cells treated with FA-PEG-SS-PEI-SPION/siScr at Fe concentrations of 10, 20, and 40 μg/mL, magnification 200×; (**B**) confocal images of SGC-7901 cells treated with FA-PEG-SS-PEI-SPION/siScr-FAM and PEG-SS-PEI-SPION/siScr-FAM.
Abbreviations: FA, folic acid; PEG, polyethylene glycol; SS, disulfide; PEI, polyethylenimine; SPION, superparamagnetic iron oxide nanoparticle; siScr-FAM, scrambled siRNA conjugated with 5-carboxyfluorescein; DAPI, 4′,6-diamidino-2-phenylindole; PP, PEG-SS-PEI-SPIONs; FP, FA-PEG-SS-PEI-SPIONs.

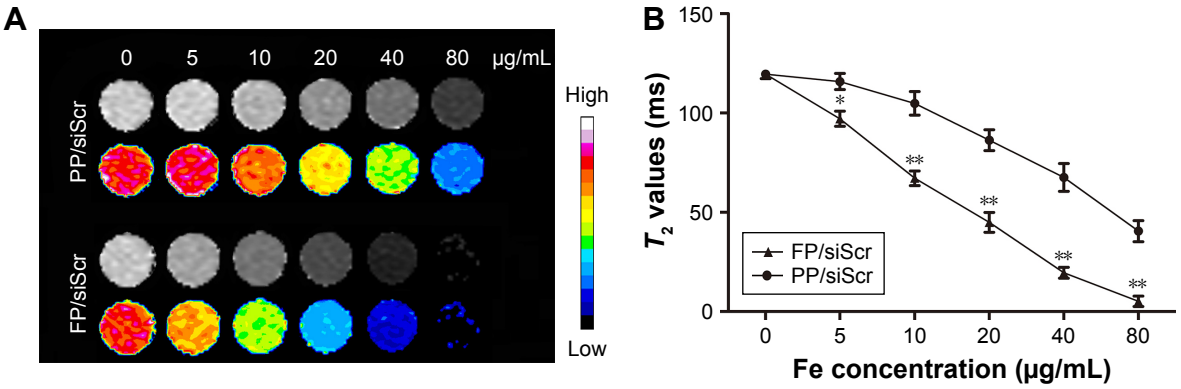

Figure 7 In vitro MRI of SGC-7901 cells.
Notes: (**A**) T_2-weighted and color T_2-mapping images and (**B**) T_2 relaxation time of SGC-7901 cells treated with PEG-SS-PEI-SPION/siScr and FA-PEG-SS-PEI-SPION/siScr at Fe concentrations of 0, 5, 10, 20, 40, and 80 μg/mL. *$P<0.05$, **$P<0.01$ versus PP/siScr (n=3).
Abbreviations: MRI, magnetic resonance imaging; FA, folic acid; PEG, polyethylene glycol; SS, disulfide; PEI, polyethylenimine; SPION, superparamagnetic iron oxide nanoparticle; siScr, scrambled siRNA; PP, PEG-SS-PEI-SPIONs; FP, FA-PEG-SS-PEI-SPIONs.

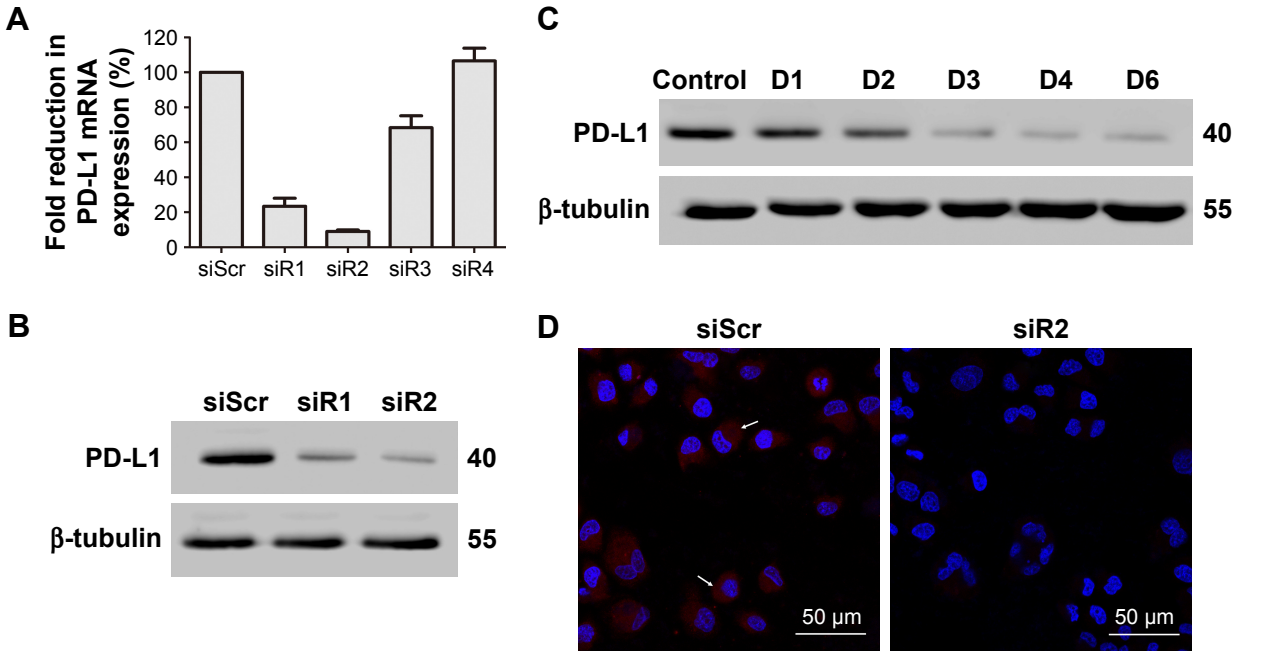

Figure 8 Knockdown of PD-L1 on SGC-7901 cells.

Notes: (**A**) mRNA levels of PD-L1 in cells treated with FA-PEG-SS-PEI-SPION/siRNA; (**B**) PD-L1 protein expression on SGC-7901 cells 72 hours post transfection, determined by Western blotting; (**C**) PD-L1 protein expression on SGC-7901 cells at days 1–6 post-transfection, determined by Western blotting; (**D**) PD-L1 protein expression on SGC-7901 cells determined by immunofluorescence analysis 72 hours post transfection. Cell nuclei were stained blue using DAPI. PD-L1 protein shown in red and indicated by arrows. Scale bar 50 μm.

Abbreviations: FA, folic acid; PEG, polyethylene glycol; SS, disulfide; PEI, polyethylenimine; SPION, superparamagnetic iron oxide nanoparticle; DAPI, 4′,6-diamidino-2-phenylindole; siScr, scrambled siRNA.

expression. Further, the knockdown effect lasted from day 3 to at least day 6 post transfection (Figure 8C). Moreover, confocal images of polymer/PD-L1 siRNA-treated SGC-7901 cells revealed much less PD-L1 expression on the cell surface than siScr-treated cells (Figure 8D). Above all, the knockdown assays confirmed that PD-L1 siRNA2 was the most efficient siRNA sequence for PD-L1 knockdown, and thus, it was used in subsequent functional experiments.

Effect of PD-L1 siRNA transfection via polyplexes on T-cell function

To determine if siRNA delivery by the polyplexes affected T-cell function via PD-L1-expression inhibition, we established an SGC-7901/T-cell coculture model. We isolated PBMCs for culture from peripheral blood samples contributed by volunteers. After coculture, the cytokine levels in the supernatants were determined with ELISAs. PD-L1-stimulating IFNγ and TNFα levels were increased, while secretion of the immunosuppressive cytokine IL10 was decreased after treatment with FA-PEG-SS-PEI-SPION/PD-L1 siRNA2 (Figure 9A–C). Consistently, incubation with functional anti-PD-L1 antibodies had similar effects. In addition, to elucidate whether treatments with FA-PEG-SS-PEI-SPION/PD-L1 siRNA reduced recruitment of regulatory T cells (T_{reg}) cells, which express CCR4,[27] the secretion of CCL22, a ligand of CCR4, was determined by ELISA. Figure 9D shows that coculture with SGC-7901 cells activated T cells to secrete more CCL22 than monocultured T cells, suggesting a T_{reg}-engaged immunosuppressive microenvironment when PD-1/PD-L1 interactions were active. In addition, treatment with FA-PEG-SS-PEI-SPION/PD-L1 siRNA or anti-PD-L1 antibodies was able partially to eliminate the increase in CCL22. Moreover, simultaneous use of FA-PEG-SS-PEI-SPION/PD-L1 siRNA and anti-PD-L1 had the most significant effect in reversing the increase in CCL22.

Discussion

PD-L1, a promising therapeutic target for advanced GCs, has been demonstrated to be a prognostic biomarker, and monoclonal antibodies specific for PD-L1 are under Phase III preclinical trials (NCT02625623, NCT02625610). Monoclonal antibodies designed to block PD-1/PD-L1 interactions have been approved for the treatment of advanced melanoma and metastatic non-small-cell lung cancer. For advanced GC, several clinical trials have confirmed that monoclonal antibodies are safe and potentially efficacious.[28,29] However, with broad expression on hematopoietic and nonhematopoietic cells,[30,31] PD-1/PD-L1 and B7-1/PD-L1 interactions regulate effector T cells and functions restraining autoimmune processes. Untargeted blockade may cause related adverse

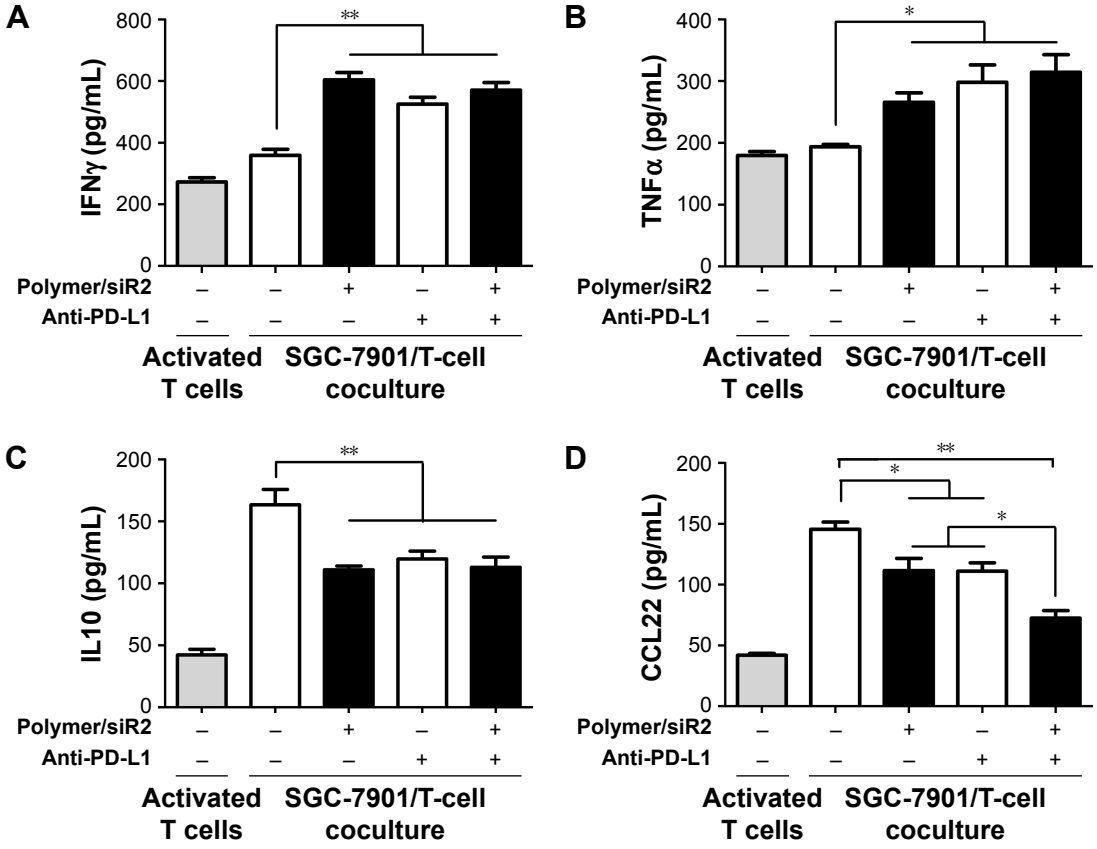

Figure 9 Cytokine secretion of SGC-7901–activated T-cell coculture.
Notes: Cytokine (**A**) IFNγ, (**B**) TNFα, (**C**) IL10, and chemokine (**D**) CCL22 concentrations in the coculture medium determined by ELISA. Results presented as mean ± SEM of three independent experiments. Student's *t*-test was used to calculate significance. *$P<0.05$; **$P<0.01$.
Abbreviations: ELISA, enzyme-linked immunosorbent assay; SEM, standard error of mean; polymer, FA-PEG-SS-PEI-SPION/PD-L1 siRNA2; FA, folic acid; PEG, polyethylene glycol; SS, disulfide; PEI, polyethylenimine; SPION, superparamagnetic iron oxide nanoparticle.

effects apart from antitumor effects whose mechanism is still not fully understood. Such effects as fatigue, decreased appetite, nausea, pruritus, dyspnea, arthralgia, and pneumonitis have been developed in trials of atezolizumab, a humanized IgG_1 monoclonal anti-PD-L1 antibody, for other PD-L1-positive cancers.[32,33] In this regard, we developed a PEI-based gene-delivery nanocarrier with SS-linked FA-PEG modification to target GC cells precisely.[17,34,35]

PEIs are highly developed as gene carriers that render high transfection efficacy of PEI/RNA polyplexes.[36,37] However, as a therapeutic gene-delivery agent, unmodified PEIs exhibit significant cytotoxicity, which restricts further application. To solve this problem, PEGylation can be used to create a hydrophilic exterior that shields the positive surface charge and stabilizes the polymers by suppressing the nonspecific interactions of PEI with blood components and the extracellular matrix.[19] With optimized PEG conjugation, the cytotoxicity of the polymers was acceptable, with N:P ratios lower than 40, while transfection efficiency remained high. In addition, to target cancer cells, FA was introduced into the delivery vector for receptor-mediated endocytosis. Because FA receptors are highly expressed in several cancers, FA can be used as a targeting group and enhance internalization by cancer cells.

SPIONs are extensively used for magnetic targeting and MRI in cancer theranostics (therapy and diagnosis), due to their magnetic properties and biodegradability.[38–40] Through positively charged polymers, such as PEIs, negatively charged nucleic acids can be conjugated with magnetic nanoparticles. This characteristic of PEI and its derivatives bridges the gap between siRNA and SPIONs, combining the functions of target-gene silencing and MRI. Ultimately, combined delivery of siRNA and SPIONs to tumor sites can improve therapeutic efficacy, reduce undesirable side effects, and provide enhanced MRI tumor contrast, which may allow the therapeutic efficiency of the treatment to be predicted based on the biodistribution of the nanomedicine and allow noninvasive monitoring of cancer progression.

Before PD-L1 knockdown, we aimed to test the cytotoxicity and transfection efficiency of various N:P ratios of the polymer/siRNA complexes to determine a suitable N:P ratio for complexation. The cytotoxicity of complexes with N:P

ratios below 20 was low, and an N:P ratio of 10 balanced low cytotoxicity and high transfection efficiency. Therefore, we used an N:P ratio of 10 for subsequent complexation and transfection experiments.

For siRNA transfection, based on flow cytometry, FA- and non-FA-modified polymers showed transfection efficiencies higher than the lipoplex control, indicating that siRNAs delivered by the agents were well internalized by most of the tumor cells. In addition, higher MFI values were observed with FA-PEG-SS-PEI-SPION/siRNA than PEG-SS-PEI-SPION/siRNA, which verified targeted uptake into SGC-7901 cells. The cellular uptake of the internalized siRNA was also observed using confocal microscopy and Prussian blue staining.

For PD-L1 knockdown, the four designed PD-L1 siRNAs were separately delivered by the nanocarriers to SGC-7901 cells. PD-L1 mRNA levels determined by qRT-PCR were decreased obviously by approximately 80% for siRNA1 and 90% for siRNA2 treatment. PD-L1 protein levels in SGC-7901 cells treated with polymer/siRNA1 or siRNA2 were much lower than those in cells treated with polymer/siScr. Protein levels were consistent with mRNA levels, which indicated that downregulation of PD-L1 was the result of the delivered PD-L1 siRNA. In sum, a target ligand-modified, T_2-weighted MR-visible polyplex, FA-PEG-SS-PEI-SPION/PD-L1 siRNA2, was used for gene-delivery knockdown of PD-L1 on SGC-7901 cells.

As a coinhibitory receptor expressed on activated T cells, PD-1 interacts with PD-L1 expressed on tumor cells. In addition, to study the change in T-cell function under treatment with polymer/PD-L1 siRNA, a coculture model of SGC-7901/T cells was established. We downregulated PD-L1 expression in SGC-7901 cells and cocultured them with activated T cells. The release of cytokines was a reflection of the T-cell function and the state of the immune microenvironment. In our study, the concentrations of cytokines in the coculture supernatants were determined by ELISA. CCL22, a CCR4-binding chemokine produced by primed $CD8^+$ effector T cells, dominates in recruiting T_{reg} cells. According to our results, PBMCs, including activated T cells, were originally a source of CCL22. However, after coculture with PD-L1-overexpressing SGC-7901 cells, CCL22 concentration was obviously increased and could be partially reversed by polymer/PD-L1 siRNA treatment. IFNγ and TNFα can be released by inflammatory cells, especially infiltrating $CD8^+$ T cells, and stimulate expression of PD-L1 on tumor cells.[27] IL10 is an immunosuppressive cytokine secreted by T cells and has been shown to be stimulated by PD-L1.[41,42] This change in cytokine secretions indicated effective PD-L1 knockdown and enhanced cytotoxic T-cell function. It has been demonstrated that $CD8^+$ T cell inflaming GCs contain high PD-L1 expression, suggesting that adaptive immune resistance is active in GC.[10] Under such an activated PD-1/PD-L1 interaction within tumors, effector T-cell functions are repressed and unable to eliminate tumor invasion. This mechanism suggested that targeting PD-1/PD-L1 interplay by siRNA delivery with FA-PEG-SS-PEI-SPIONs could yield effective clinical outcomes in GC.

Conclusion

We synthesized and characterized a gene-delivery system based on SPIONs encapsulated with FA-PEG-SS-PEI polymer and successfully delivered PD-L1 siRNA into SGC-7901 cells. The FA-PEG-SS-PEI-SPION/siRNA polyplex exhibited low cytotoxicity and significant cellular uptake. The polyplex showed capability to act as a nanoprobe for cancer MRI and enhance cellular T_2-weighted contrast. In addition, cellular internalization of the polyplex resulted in PD-L1 downregulation at both the mRNA and protein levels, and thus affected cytokine-secretion levels of cocultured T-cells. In summary, the FA-PEG-SS-PEI-SPION/PD-L1 siRNA polyplex shows MRI tracing capability and efficient PD-1/PD-L1 blockade in vitro, which highlights the significant theranostic potential of these nanocarriers and their potential ability to restore T-cell immune response in GCs.

Acknowledgments

We would like to thank Lu Zhang, PhD from the School of Chemistry and Chemical Engineering, Sun Yat-sen University, Guangzhou, China, for kindly providing technical support for chemical synthesis of the polymer nanocarrier.

Disclosure

The authors report no conflicts of interest in this work.

References

1. Torre LA, Siegel RL, Ward EM, Jemal A. Global cancer incidence and mortality rates and trends: an update. *Cancer Epidemiol Biomarkers Prev*. 2016;25(1):16–27.
2. Jemal A, Bray F, Center MM, Ferlay J, Ward E, Forman D. Global cancer statistics. *CA Cancer J Clin*. 2011;61(2):69–90.
3. Zou W, Chen L. Inhibitory B7-family molecules in the tumour microenvironment. *Nat Rev Immunol*. 2008;8(6):467–477.
4. Francisco LM, Salinas VH, Brown KE, et al. PD-L1 regulates the development, maintenance, and function of induced regulatory T cells. *J Exp Med*. 2009;206(13):3015–3029.
5. Paterson AM, Brown KE, Keir ME, et al. The programmed death-1 ligand 1:B7-1 pathway restrains diabetogenic effector T cells in vivo. *J Immunol*. 2011;187(3):1097–1105.

6. Butte MJ, Keir ME, Phamduy TB, Sharpe AH, Freeman GJ. Programmed death-1 ligand 1 interacts specifically with the B7-1 costimulatory molecule to inhibit T cell responses. *Immunity*. 2007;27(1):111–122.
7. Wang W, Li F, Mao Y, et al. A miR-570 binding site polymorphism in the B7-H1 gene is associated with the risk of gastric adenocarcinoma. *Hum Genet*. 2013;132(6):641–648.
8. Savabkar S, Azimzadeh P, Chaleshi V, Mojarad EN, Aghdaei HA. Programmed death-1 gene polymorphism (PD-1.5 C/T) is associated with gastric cancer. *Gastroentero Hepatol Bed Bench*. 2013;6(4):178–182.
9. Saito H, Kuroda H, Matsunaga T, Osaki T, Ikeguchi M. Increased PD-1 expression on CD4+ and CD8+ T cells is involved in immune evasion in gastric cancer. *J Surg Oncol*. 2013;107(5):517–522.
10. Thompson ED, Zahurak M, Murphy A, et al. Patterns of PD-L1 expression and CD8 T cell infiltration in gastric adenocarcinomas and associated immune stroma. *Gut*. 2017;66(5):794–801.
11. Zhang L, Qiu M, Jin Y, et al. Programmed cell death ligand 1 (PD-L1) expression on gastric cancer and its relationship with clinicopathologic factors. *Int J Clin Exp Pathol*. 2015;8(9):11084–11091.
12. Hou J, Yu Z, Xiang R, et al. Correlation between infiltration of FOXP3+ regulatory T cells and expression of B7-H1 in the tumor tissues of gastric cancer. *Exp Mol Pathol*. 2014;96(3):284–291.
13. Lu B, Chen L, Liu L, et al. T-cell-mediated tumor immune surveillance and expression of B7 co-inhibitory molecules in cancers of the upper gastrointestinal tract. *Immunol Res*. 2011;50(2–3):269–275.
14. Liu SM, Meng Q, Zhang QX, Wang SD, Liu ZJ, Zhang XF. [Expression and significance of B7-H1 and its receptor PD-1 in human gastric carcinoma]. *Zhonghua Zhong Liu Za Zhi*. 2008;30(3):192–195. Chinese.
15. Wu C, Zhu Y, Jiang J, Zhao J, Zhang XG, Xu N. Immunohistochemical localization of programmed death-1 ligand-1 (PD-L1) in gastric carcinoma and its clinical significance. *Acta Histochem*. 2006;108(1):19–24.
16. Cancer Genome Atlas Research Network. Comprehensive molecular characterization of gastric adenocarcinoma. *Nature*. 2014;513(7517):202–209.
17. Ma H, Liu Y, Shi M, et al. Theranostic, pH-responsive, doxorubicin-loaded nanoparticles inducing active targeting and apoptosis for advanced gastric cancer. *Biomacromolecules*. 2015;16(12):4022–4031.
18. Godbey WT, Wu KK, Mikos AG. Poly(ethylenimine) and its role in gene delivery. *J Control Release*. 1999;60(2–3):149–160.
19. Li L, Wei Y, Gong C. Polymeric nanocarriers for non-viral gene delivery. *J Biomed Nanotechnol*. 2015;11(5):739–770.
20. Wang S, Low PS. Folate-mediated targeting of antineoplastic drugs, imaging agents, and nucleic acids to cancer cells. *J Control Release*. 1998;53(1–3):39–48.
21. Sudimack J, Lee RJ. Targeted drug delivery via the folate receptor. *Adv Drug Deliv Rev*. 2000;41(2):147–162.
22. Sun S, Zeng H, Robinson DB, et al. Monodisperse MFe_2O_4 (M = Fe, Co, Mn) nanoparticles. *J Am Chem Soc*. 2004;126(1):273–279.
23. Lee H, Jeong JH, Park TG. A new gene delivery formulation of polyethylenimine/DNA complexes coated with PEG conjugated fusogenic peptide. *J Control Release*. 2001;76(1–2):183–192.
24. Liang B, He ML, Chan CY, et al. The use of folate-PEG-grafted-hybranched-PEI nonviral vector for the inhibition of glioma growth in the rat. *Biomaterials*. 2009;30(23–24):4014–4020.
25. Cammas S, Nagasaki Y, Kataoka K. Heterobifunctional poly(ethylene oxide): synthesis of α-methoxy-ω-amino and α-hydroxy-ω-amino PEOs with the same molecular weights. *Bioconjug Chem*. 1995;6(2):226–230.
26. Tromsdorf UI, Bigall NC, Kaul MG, et al. Size and surface effects on the MRI relaxivity of manganese ferrite nanoparticle contrast agents. *Nano Lett*. 2007;7(8):2422–2427.
27. Spranger S, Spaapen RM, Zha Y, et al. Up-regulation of PD-L1, IDO, and T_{regs} in the melanoma tumor microenvironment is driven by $CD8^+$ T cells. *Sci Transl Med*. 2013;5(200):200ra116.
28. Muro K, Chung HC, Shankaran V, et al. Pembrolizumab for patients with PD-L1-positive advanced gastric cancer (KEYNOTE-012): a multicentre, open-label, phase 1B trial. *Lancet Oncol*. 2016;17(6):717–726.
29. Brahmer JR, Tykodi SS, Chow LQ, et al. Safety and activity of anti-PD-L1 antibody in patients with advanced cancer. *N Engl J Med*. 2012;366(26):2455–2465.
30. Keir ME, Butte MJ, Freeman GJ, Sharpe AH. PD-1 and its ligands in tolerance and immunity. *Annu Rev Immunol*. 2008;26:677–704.
31. Freeman GJ, Long AJ, Iwai Y, et al. Engagement of the PD-1 immunoinhibitory receptor by a novel B7 family member leads to negative regulation of lymphocyte activation. *J Exp Med*. 2000;192(7):1027–1034.
32. Rosenberg JE, Hoffman-Censits J, Powles T, et al. Atezolizumab in patients with locally advanced and metastatic urothelial carcinoma who have progressed following treatment with platinum-based chemotherapy: a single-arm, multicentre, phase 2 trial. *Lancet*. 2016;387(10031):1909–1920.
33. Fehrenbacher L, Spira A, Ballinger M, et al. Atezolizumab versus docetaxel for patients with previously treated non-small-cell lung cancer (POPLAR): a multicentre, open-label, phase 2 randomised controlled trial. *Lancet*. 2016;387(10030):1837–1846.
34. Cui D, Zhang C, Liu B, et al. Regression of gastric cancer by systemic injection of RNA nanoparticles carrying both ligand and siRNA. *Sci Rep*. 2015;5:10726.
35. Huang P, Bao L, Zhang C, et al. Folic acid-conjugated silica-modified gold nanorods for X-ray/CT imaging-guided dual-mode radiation and photo-thermal therapy. *Biomaterials*. 2011;32(36):9796–9809.
36. Jäger M, Schubert S, Ochrimenko S, Fischer D, Schubert US. Branched and linear poly(ethylene imine)-based conjugates: synthetic modification, characterization, and application. *Chem Soc Rev*. 2012;41(13):4755–4767.
37. Kichler A, Leborgne C, Coeytaux E, Danos O. Polyethylenimine-mediated gene delivery: a mechanistic study. *J Gene Med*. 2001;3(2):135–144.
38. Bakhtiary Z, Saei AA, Hajipour MJ, Raoufi M, Vermesh O, Mahmoudi M. Targeted superparamagnetic iron oxide nanoparticles for early detection of cancer: possibilities and challenges. *Nanomedicine*. 2016;12(2):287–307.
39. Kandasamy G, Maity D. Recent advances in superparamagnetic iron oxide nanoparticles (SPIONs) for in vitro and in vivo cancer nanotheranostics. *Int J Pharm*. 2015;496(2):191–218.
40. Yen SK, Padmanabhan P, Selvan ST. Multifunctional iron oxide nanoparticles for diagnostics, therapy and macromolecule delivery. *Theranostics*. 2013;3(12):986–1003.
41. Dennis KL, Blatner NR, Gounari F, Khazaie K. Current status of interleukin-10 and regulatory T-cells in cancer. *Curr Opin Oncol*. 2013;25(6):637–645.
42. Dong H, Zhu G, Tamada K, Chen L. B7-H1, a third member of the B7 family, co-stimulates T-cell proliferation and interleukin-10 secretion. *Nat Med*. 1999;5(12):1365–1369.